5-2013

Mathematical Modeling of Two-Phase Arterial Blood Flow

Ani Emire Garcia Escorcia
University of Texas-Pan American

MATHEMATICAL MODELING OF TWO-PHASE ARTERIAL BLOOD FLOW

A Thesis

by

ANI EMIRE GARCIA ESCORCIA

Submitted to the Graduate School of the
University of Texas-Pan American
In partial fulfillment of the requirements for the degree of

MASTER OF SCIENCE

May 2013

Major Subject: Mathematical Science

MATHEMATHICAL MODELING OF TWO-PHASE ARTERIAL BLOOD FLOW

A Thesis
by
ANI EMIRE GARCIA ESCORCIA

COMMITTEE MEMBERS

Dr. Daniel Riahi
Chair of Committee

Dr. Ranadhir Roy
Committee Member

Dr. Anahit Galstyan
Committee Member

Dr. Paul Bracken
Committee Member

May 2013

ABSTRACT

Garcia Escorcia, Ani Emire. Mathematical Modeling of Two-Phase Arterial Blood Flow. Master of Science (MS), May, 2013, 38 pp., 26 figures, references, 6 titles.

Problem of blood flow in an artery with or without catheter and in the presence of single or multi stenosis will be considered. The presence of stenosis locally thickens the artery wall and the use of catheter in the affected area is very important to the diagnostic and treatment of the patient. The blood flow in the arterial tube is represented by a two-phase model composing a suspension of erythrocytes in plasma. The governing equations for both fluid and particles are solved subjected to reasonable modeling and approximations. The important quantities such as blood speed, blood pressure force, impedance (blood flow resistance), wall shear stress, the stress force, blood temperature and the heat flux on the artery are computed in the presence or absence of the catheter and in the presence of the axially located stenosis, gravity and the hematocrit due the red cells-plasma combination of the blood flow.

DEDICATION

The completion of my master degree and everything I have done would not be possible without the support and love of my family. Thank you to my mother, Maria Dolores, and my father Carlos Garcia for giving me the chance to continue with my studies. Thank you for all your love, dedication, and patience.

ACKNOWLEDGMENTS

I will always be grateful to Dr. Daniel Riahi, chair of my thesis committee, for all his help in completing my thesis. He was always willing to help me. Thank you, Dr. Riahi for your patience and help.

Also, I want to thank my thesis committee members: Dr. Roy, Dr. Galstyan and Dr. Bracken for their help, and advices in completing my thesis.

TABLE OF CONTENTS

LIST OF FIGURES

CHAPTER I

INTRODUCTION

Diseases in the blood vessels and in the heart, such as heart attack and stroke, are the major causes of mortality worldwide. The underlying cause of these events is the formation of lesions, known as stenosis. These lesions and plaques can grow and occlude the artery and hence prevent blood supply to the distal bed. Plaques with calcium in them can also rupture and initiate the formation of blood clots known also as thrombus. Theses clots can form as emboli and occlude the smaller vessels that can also result in interruption of blood supply to distal bed. Also, plaques formed in coronary arteries can lead to heart attacks and clots in the cerebral circulation can result in the stroke. There are number of risk factors for the presence of stenosis. The common sites for the formations of stenosis include the coronary arteries, the branching of the subclavian and common carotids especially in the carotid sinus region distal to the bifurcations, the renal arterial branching in the descending aorta and in the ileofemoral bifurcations of the descending aorta. The common feature in the location for the development of the lesion is the presence of curvature, branching and bifurcation present in these sites. The fluid dynamics at these sites can be anticipated to be vastly different from other segments of the arteries that are relatively straight and devoid of any branching segments.

CHAPTER II

REVIEW OF LITERATURE

Several investigators have attempted to link the fluid dynamically induced stress with the formation of stenosis in the human circulation. By assuming the artery to be circularly in shape, Mishra (2003) discussed characteristics of blood in stenosed artery and the stenosis to be symmetric about the axis of artery. Mishra and Panda (2005) studied the flow of blood in stenosed artery for the Casson type fluid. Young and Tsai (1973) discussed some characteristics of flow of blood in stented arteries. Venkateswarlu and Rao (2004) studied and assumed oscillatory form of the blood flow through an indented tube in presence of steady single stenosis with a very simple shape. They used the so-called Einstein model for the viscosity of the blood but for variable volume flow rate and the prescribed value for the magnitude of the pressure gradient. Riahi (2011) investigated arterial blood flow in the presence of an overlapping stenosis using the variable viscosity model due to Einstein for the blood flow.

In this study, an experimental based shape for the atherosclerosis shape in the artery is applied (Figure 1), where the blood is represented by a two-phase macroscopic model. Figure 1 and Figure 2 show dimensional shape function R(z) of multi-stenosis and single stenosis respectively versus dimensional value of the axial variable of an artery based on the actual dimensional data determined from the experimental values of the cross-sectional area of the artery of a human (Back et al., 1984). Here and as in the more realistic cases, the blood flow is composed of a suspension of erythrocytes in plasma. I also include the presence of gravity and prescribe temperature on the surface of the artery in order to determine information effects of gravity as well as presence of temperature in the blood flow and the total heat flux in the arterial blood flow system. (Garcia, Riahi 2013)

CHAPTER III

METHODOLOGY AND FINDINGS

Methodology and findings for single and multi-stenosis in artery

I consider the problem of axisymmetric flow of blood in catheterized artery in the form of a circular cylindrical annulus tube with the outer radios R_0 (radius of the artery) and the inner radius r_1 (radius of the catheter) and in the presence of single or multi-stenosis whose shape is determined from the experimentally collected data (Back et al., 1984). Also, arterial blood flow in the absence of catheter (r_1=0) is considered.

The two-phase flow system in artery is based on the original governing equations for the mass conservation and momentum (Batchelor, 1970) for both fluid plasma and the suspended particles as their steady axisymmetric form in cylindrical coordinate system with axial direction along the co-axial direction of the catheterized artery are given by (Sirvastava and Rastogi, 2010)

$$(1-C)\rho_f\left(u_f\frac{\partial u_f}{\partial z}+v_f\frac{\partial u_f}{\partial r}\right)=-(1-C)\frac{\partial P}{\partial z}+(1-C)\mu_s\nabla^2 u_f+CS'(u_p-u_f) \tag{1a}$$

$$(1-C)\rho_f\left(u_f\frac{\partial v_f}{\partial z}+v_f\frac{\partial v_f}{\partial r}\right)=-(1-C)\frac{\partial P}{\partial r}+(1-C)\mu_s(\nabla^2-\frac{1}{r^2})v_f+CS'\left(v_p-v_f\right) \tag{1b}$$

$$\frac{1}{r}\frac{\partial}{\partial r}[(1-C)v_f]+\frac{\partial}{\partial z}[(1-C)u_f]=0 \tag{1c}$$

$$C\rho_p\left[u_p\frac{\partial u_p}{\partial z}+v_p\frac{\partial u_p}{\partial r}\right]=-\frac{\partial P}{\partial z}+CS'\left(u_f-u_p\right) \tag{1d}$$

$$C\rho_p\left[u_p\frac{\partial v_p}{\partial z}+v_p\frac{\partial v_p}{\partial r}\right]=-\frac{\partial P}{\partial z}+CS'\left(v_f-v_p\right) \tag{1e}$$

$$\frac{1}{r}\frac{\partial}{\partial r}(Crv_{p)}+\frac{\partial}{\partial z}\left(Cu_p\right)=0 \tag{1f}$$

Where $\nabla^2\equiv\frac{1}{r}\frac{\partial}{\partial r}\left(r\frac{\partial}{\partial r}\right)+\frac{\partial^2}{\partial z^2}$ is the Laplace operator. Here r ($r_1\leq r\leq R_0$) and z are the cylindrical coordinates with the axial variable z along the tube axis and radial variable r along the direction perpendicular to the tube axis. Also, u is the axial velocity component, v is the radial velocity component, f and p are the fluid (plasma) and particle quantities (red cells), ρ is the density, P is pressure; C is the hematocrit % in the blood. Formulas for viscosity of suspension μ_s and drag coefficient of interaction S' are also needed (Srivastava, 1996; Srivastava,2009)

$$\mu_s=\frac{\mu_0}{(1-mC)},\ m=0.07e^{2.49C+\frac{1107}{T}e^{-1.69C}} \tag{1g}$$

$$S^{'}=4.5\frac{\mu_0}{a_0^2}\left(\frac{4+3\sqrt{8C-3C^2}+3C}{(2-3C)^2}\right) \tag{1h}$$

Where μ_0 is the plasma viscosity, a_0 is radius of a red cell and T is the absolute temperature in Kelvin. Formula (1g) represents classical stokes drag valid for small particle Reynolds number and was first derived by Tam (1969) and is accurate up to 60% of hematocrit (Charm and Kurland 1974).

The inside of the boundary of the artery is partially structured within and axial distance L_0 due to the presence of the stenosis. Figure 1 shows the geometry of the artery with multi-stenosis on (z, r) plane in the absence of the catheter, also the flow system and the geometry is shown in the cylindrical tube over a distance $L=3d+2L_0$ in the axial direction. It is important to consider the maximum height of each stenosis into the lumen, δ. And also we will consider a value very close to the maximum height, this will be the critical height of the stenosis at a distance $z=d+L_0/2$ from the origin.

Equations (1a-h) need to be made dimensionless. U, L_0, R_0, δ and $\mu_0 U L_0/\delta^2$ are going to be used where U is the maximum velocity (White, 1991), L_0 is the axial length, R_0 is the radial length, δ and $\mu_0 U L_0/\delta^2$ are the rate of radial change and pressure respectively. Next, simplify the dimensionless forms of the equations under the reasonable conditions for mild stenosis with $\delta/R_0 \ll 1$, unidirectional flow assumption (White, 1991) where the axial velocity component dominates over the radial velocity component, and subjected to the assumptions that the inertial terms in the governing momentum equations (1a-b, d-e) are small and $R_e(\delta/L_0) \ll 1$. Under these conditions and assumptions (Srivastava and Rastogi, 2010), the pressure is only a function of z and (1a-h) lead to simpler equations:

$$(1\text{-c})\frac{dP}{dz}=\frac{1-C}{1-mC}\left[\frac{1}{r}\frac{\partial}{\partial r}\left(r\frac{\partial u_f}{\partial r}\right)\right]+CS\beta^2\left(u_p-u_f\right) \tag{2a}$$

$$\frac{dP}{dz}=S\beta^2\left(u_f-u_p\right) \tag{2b}$$

$$S=4.5\left(\frac{4+3\sqrt{8C-3C^2}+3C}{(2-3C)^2}\right)$$

where $\beta=\delta/a_0$. For equations (2a-b), consider the following no slip boundary conditions which hold in the presence of catheter:

$$u_f=0 \text{ on } r=r_1 \text{ and } u_f=0 \text{ on } r=R(z), \tag{2c}$$

and

$$\partial u_f/\partial z=0 \text{ at } r=0 \text{ and } u_f=0 \text{ on } r=R(z) \tag{2d}$$

in the absence of the catheter.

Using (2b) for (u_f-u_p) in (2a) and integrating twice with respect to r and making use of the boundary conditions given in (2c), we find that in the presence of catheter

$$u_f=\left(\frac{-1}{4}\right)\left(\frac{1-mC}{1-C}\right)\frac{dP}{dz}\left[\left(R^2-r^2\right)+\frac{\left(R^2-r_1^2\right)\ln\left(\frac{r}{R}\right)}{\ln\left(\frac{R}{r_1}\right)}\right] \tag{3a}$$

and the expression for the axial velocity for the red cells is found using (2b) in terms of axial velocity for the plasma:

$$u_p = u_f - \left(\frac{1}{S\beta^2}\right)\left(\frac{dP}{dz}\right) \tag{3b}$$

In the absence of the catheter the results are found to be:

$$u_p = u_f - \left(\frac{1}{S\beta^2}\right)\left(\frac{dP}{dz}\right) \tag{3b}$$

and

$$u_f = \left(\frac{1}{4}\right)\left(\frac{1-mC}{1-C}\right)\left(\frac{dP}{dz}\right)\left(r^2-R^2\right) \tag{3c}$$

Expressions for the axial velocity of plasma and red cells given by (3a-c) are in terms of the pressure gradient denoted by dP/dz which can be solved if we use equations (3a-c) and if we assume a prescribe volume flow in the annulus given by

$$Q = 2\pi \int_{r_1}^{R} r\left[(1-C)u_f + Cu_p\right]dr \tag{4}$$

Thus, we find an expression for the pressure gradient which is given by

$$\frac{dP}{dz} = \frac{-Q}{\left(\frac{\pi}{16}\right)\left(R^2-r_1^2\right)\left\{\left(\frac{16C}{S\beta^2}\right)+2\left(\frac{R^2-r_1^2}{1-C}\right)(1-mC)\left[\frac{R^2+r_1^2}{R^2-r_1^2}-\frac{1}{\ln\left(\frac{R}{r_1}\right)}\right]\right\}} \tag{5a}$$

which holds in the presence of the catheter, and in the absence of the catheter we have

$$\frac{dP}{dz} = \frac{-Q}{\left(\frac{\pi}{16}\right)\left(R^2\right)\left\{\left(\frac{16C}{S\beta^2}\right)+2\left(R^2\right)\left(\frac{1-mC}{1-C}\right)\right\}} \tag{5b}$$

The flow resistance, referred to as the impedance λ, is given by

$$\lambda = \Delta P/Q, \tag{6a}$$

where Δp is the pressure drop across the length L=1+2b for single stenosis case or L=2+3b for multi stenosis given by

$$\Delta P = P(0) - P(L) = \int_0^L \frac{dP}{dz} dz \tag{6b}$$

and $b=d/L_0$.

From (3a), we find the wall shear stress τ_w to be

$$\tau_w = -\frac{\partial u_f}{\partial r}\Big|_{r=R(z)} = -\frac{R(1-mC)}{2(1-C)}\frac{dP}{dz} - \left(\frac{1}{4R}\right)\left(\frac{1-mC}{1-C}\right)\frac{dP}{dz}\left[\frac{r_1{}^2 - R^2}{\ln\left(\frac{R}{r_1}\right)}\right] \tag{7a}$$

for the case where the catheter is present in the artery, and in the absence of catheter we find from (3c) the following result:

$$\tau_w = -\frac{R(1-mC)}{2(1-C)}\frac{dP}{dz} \tag{7b}$$

and the shear stress force F over surface of the artery from z=0 to z=L=1+2b for single stenosis case or z=L=2+3b for the multi stenosis case is then given by

$$F = 2\pi \int_0^L \tau_w dz \tag{7c}$$

Calculations using the previous expressions are introduced for different values of hematocrit C, and different values for radius of catheter, and in the absence of catheter. For all calculations, Q=1, b=0.5, and β=δ/0.004 where δ=1-minimum value of R.

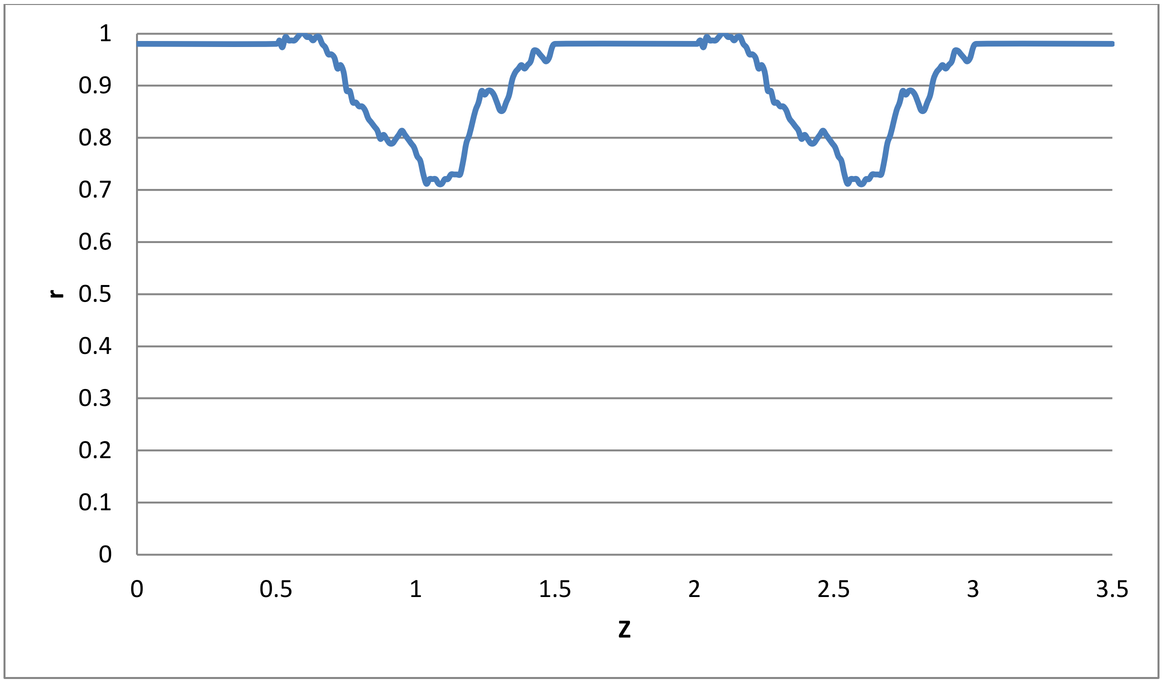

Figure 1. Geometrical view of the arterial segment with multi-stenosis.

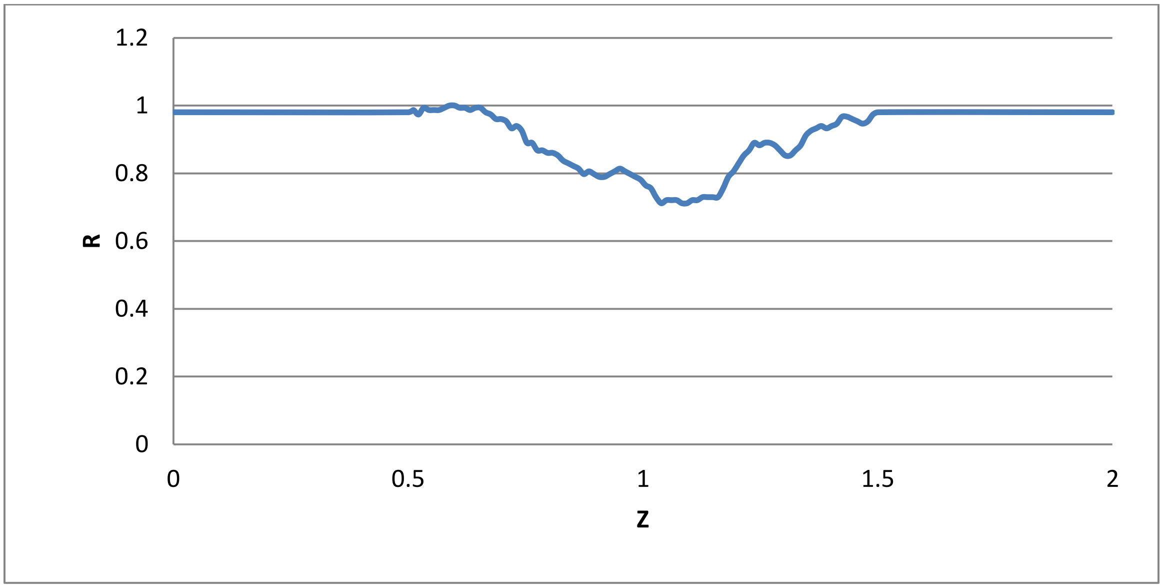

Figure 2. Shape of stenosis in the artery (single stenosis)

Figure 3 represents the pressure gradient dP/dz versus the axial variable *z* for single stenosis where C=0.1 was used as the hematocrit and for absence (r_1=0) and presence of catheter (r_1=0.1 and 0.3). From this figure, one can notice that the blood pressure gradient is negative which makes sense since the blood pressure force is in the positive direction of the z-axis. Also, the magnitude of pressure gradient increases with the effect due to the presence of the catheter which intensifies notably under the stenosis location. Outside the stenosis zone, the pressure gradient does not change. These results are reasonable since the presence of catheter can intensify the blood pressure force in the artery when there is more severe stenosis.

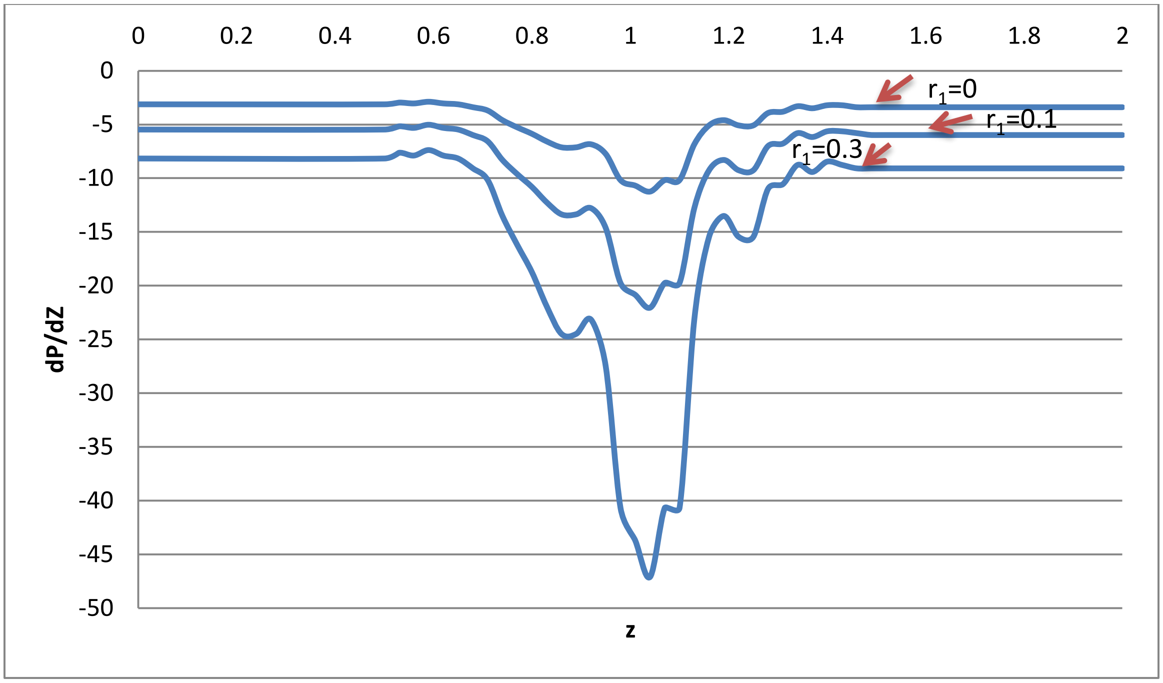

Figure 3. Pressure gradient versus axial variable for single stenosis case, C=0.1 and several values of r_1=0, 0.1, 0.3 for cases with or without catheter.

Figure 4 shows the same as figure 3 but now with hematocrit parameter C=0.5. Comparing figure 3 and 4, one can notice that the pressure gradient increases with the hematocrit parameter for the case of presence of catheter with radius r_1=0.3. This result is also reasonable since the pressure driven force is higher for higher percentage of red cells in the plasma.

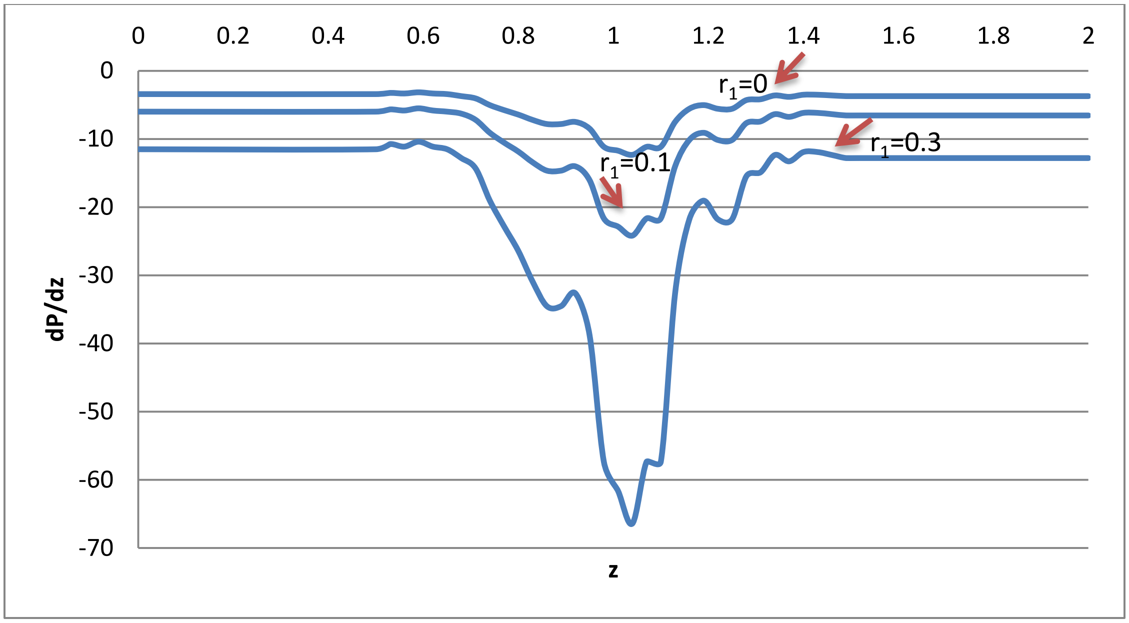

Figure 4. Pressure gradient versus axial variable for single stenosis case, *C*=0.5 and several values of r_1=0, 0.1, 0.3 for cases with or without catheter.

Figure 5 and figure 6 shows pressure gradient now for multi-stenosis for C=0.1 and C=0.5 respectively with different values of radius for catheter, r_1=0, 0.1 and 0.3.

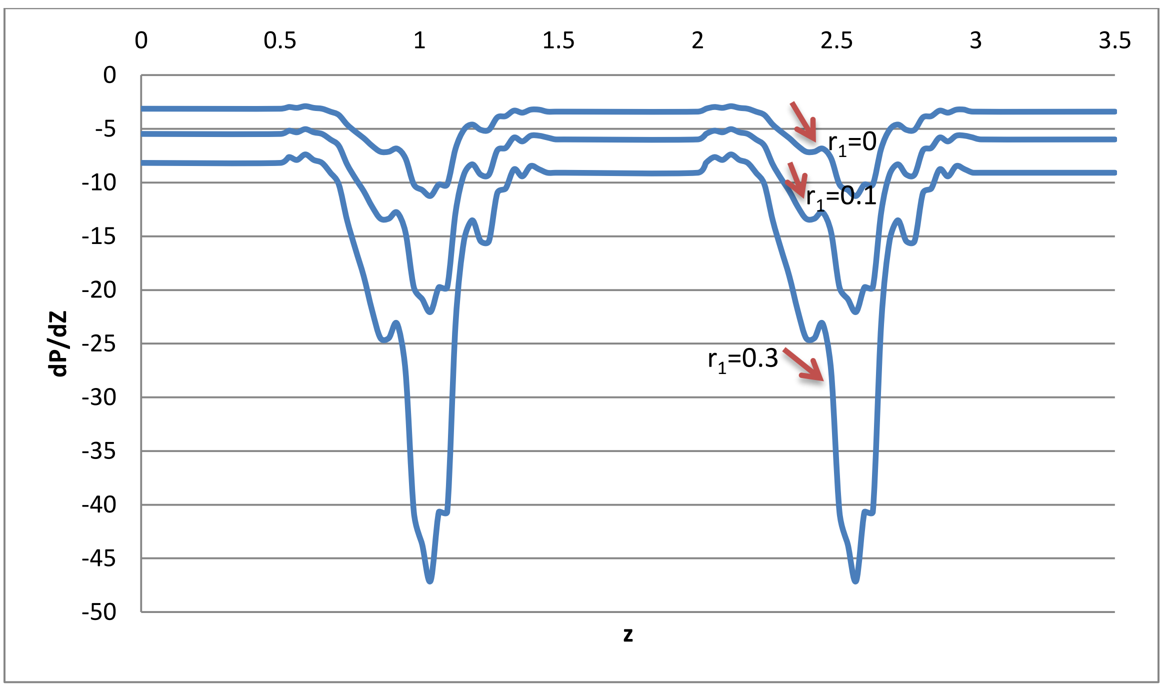

Figure 5. Pressure gradient versus z for hematocrit C=0.1 with multi-stenosis

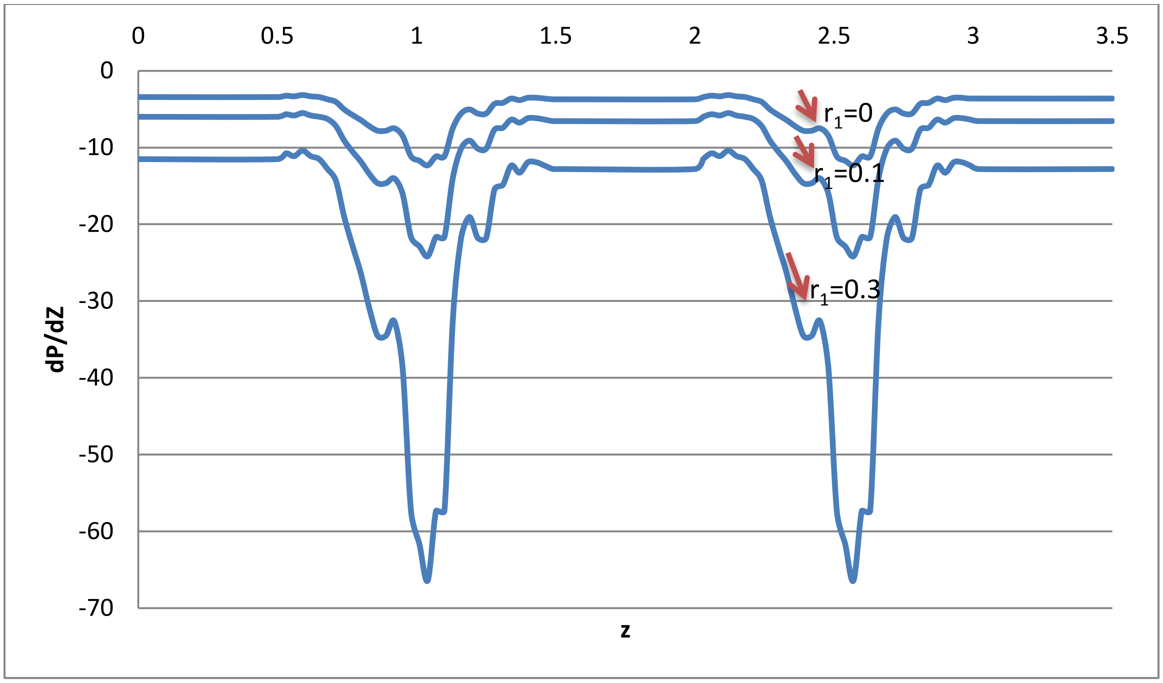

Figure 6. Pressure gradient versus z for hematocrit C=0.5 with multi-stenosis

Figure 7 shows the impedance also known as flow resistance versus hematocrit in the absence or presence of catheter. This figure shows that impedance increases with hematocrit, and it also increases with the presence of catheter. There is a small flow resistance when there is no catheter in artery. It can also be seen that for very small or large values of hematocrit, the rate of increase of the flow resistance is higher.

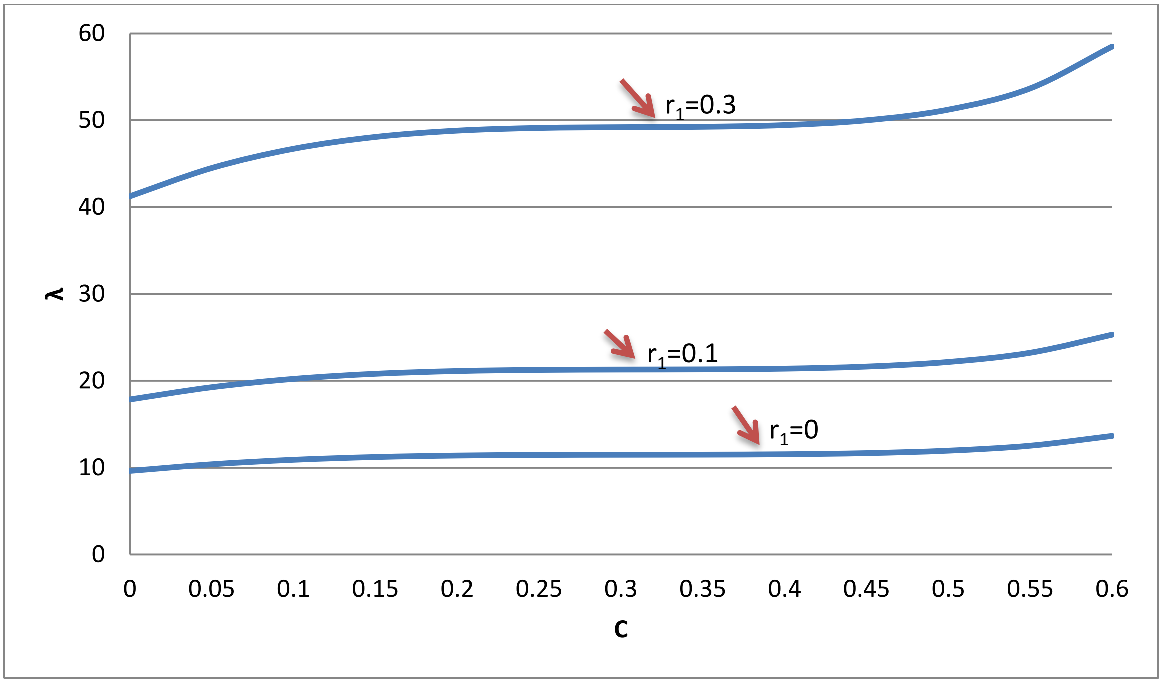

Figure 7. Impedance λ versus *C* for r_1=0, 0.1, 0.3 for single stenosis and with or without catheter.

Figure 8 shows the same as figure 7, impedance versus hematocrit but now in the presence of multi-stenosis. It can be seen that the impedance is significantly large when multi-stenosis in the artery. It also shows that for absence of catheter, impedance is low compared to impedance when catheter is inserted into the artery. Similarly as in figure 7, for very small and very large values of hematocrit, the rate of increase of the impedance is higher.

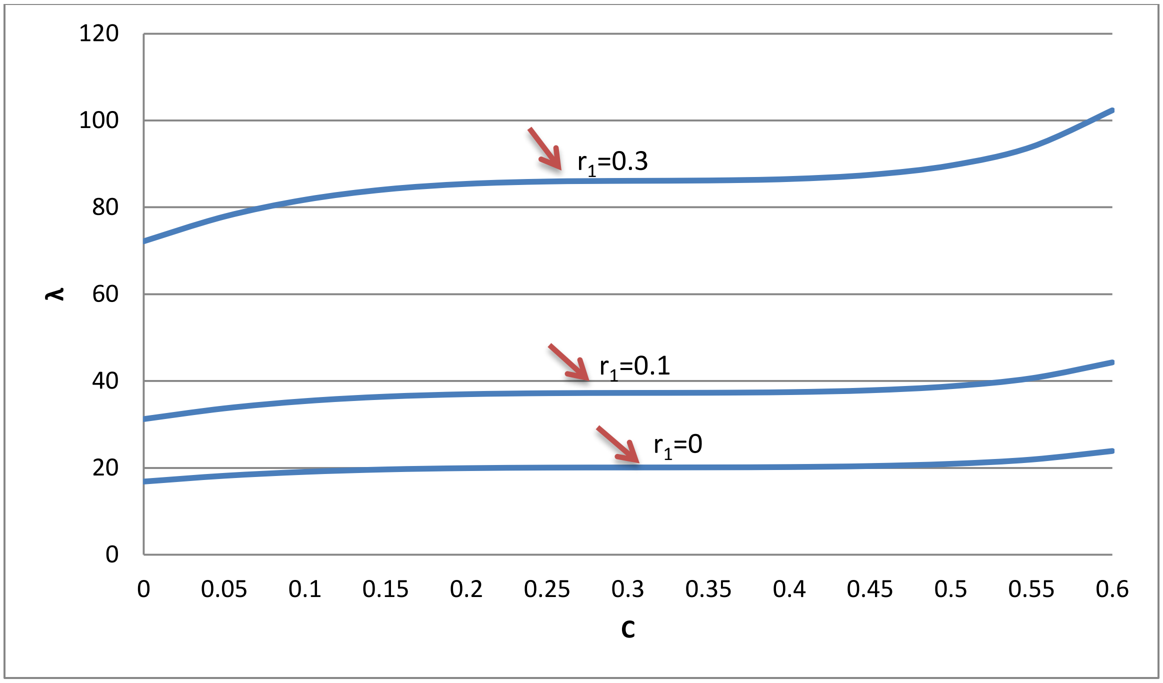

Figure 8. Impedance λ versus *C* for r_1=0, 0.1, 0.3 for multi-stenosis and with or without catheter.

In the following figures 9 and 10, axial velocity of the blood plasma u_f, versus the axial variable *z* for r=0.5 are considered, with different hematocrit parameters C=0.1, 0.5 respectively, for multi-stenosis and in the presence or absence of catheter. It can be seen that plasma velocity does not vary outside the stenosis zone; however its magnitude increases with the stenosis effect. Also, plasma velocity is positive since the blood pressure force is in the positive direction of the axis of the artery system. Bio-medically, this is reasonable since for higher stenosis, the pressure force increases leading to higher blood plasma speed. It can also be seen from the figures that the plasma velocity increases significantly with larger radius of catheter. Plasma velocity also increases with the hematocrit parameter.

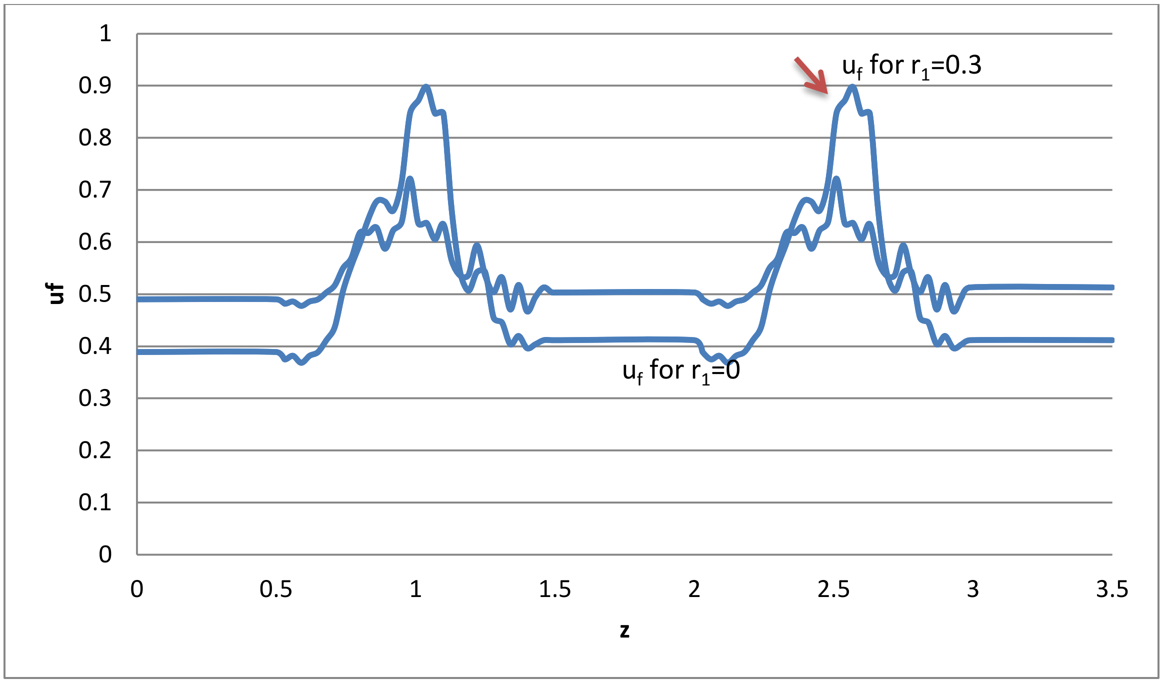

Figure 9. Plasma velocity versus axial variable at *r* =0.5 for multi stenosis, *C*=0.1 and for cases with or without catheter.(r_1=0, 0.3).

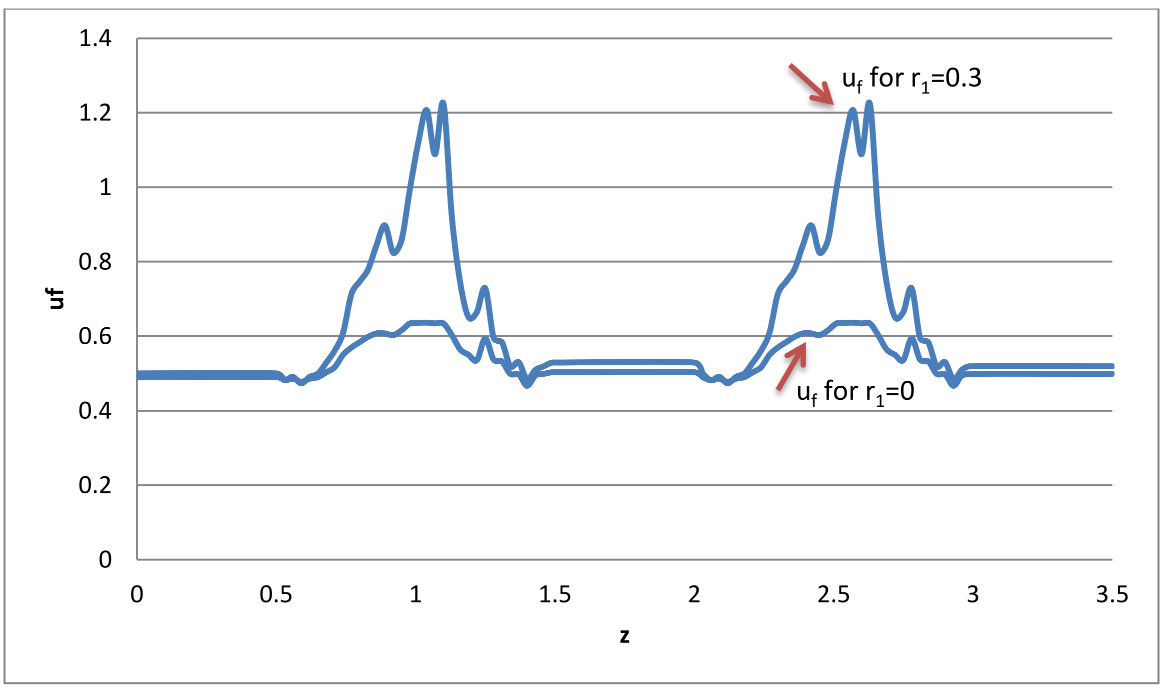

Figure 10. Plasma velocity versus axial variable at *r* =0.5 for multi stenosis, *C*=0.5 and for cases with or without catheter.(r_1=0, 0.3).

Figure 11 shows plasma velocity versus radial variable where z=2.5, hematocrit parameter C=0.5 and in the absence of catheter (r_1=0). It can be seen from this figure that plasma velocity decreases with increasing the radial variable. The rate of decrease of the plasma speed is higher close to upper values of *r* close to the stenosis zone. Also, plasma velocity is zero at r=R(z), so it satisfies the no slip boundary conditions.

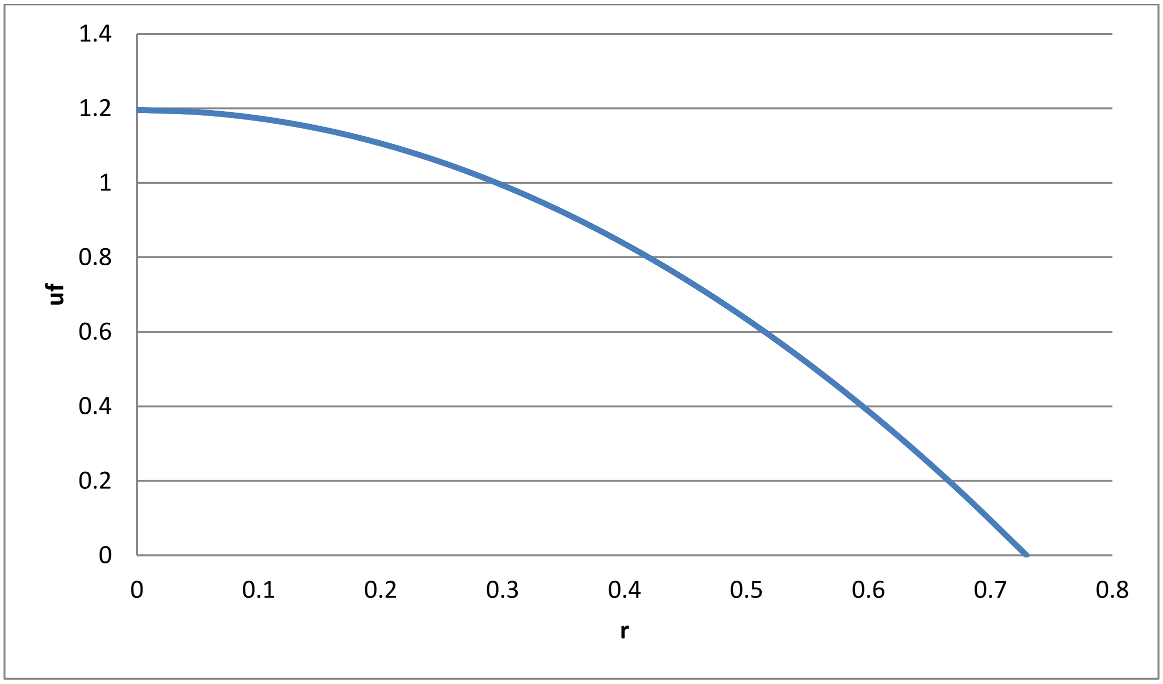

Figure 11. Plasma velocity versus radial variable for multi stenosis, z=2.5, C=0.5, r_1=0.

Figure 12 shows also plasma velocity versus radial variable for the same parameters as in figure 12 but now in the presence of catheter with radius of 0.3 (r_1=0.3). It can be seen that, plasma velocity has its maximum value at some point in the annulus away from the boundary. It also satisfies its zero no slip boundary conditions of the catheterized artery system. Comparing the two figures, one can see that plasma velocity decreases radially when catheter is used in the patient.

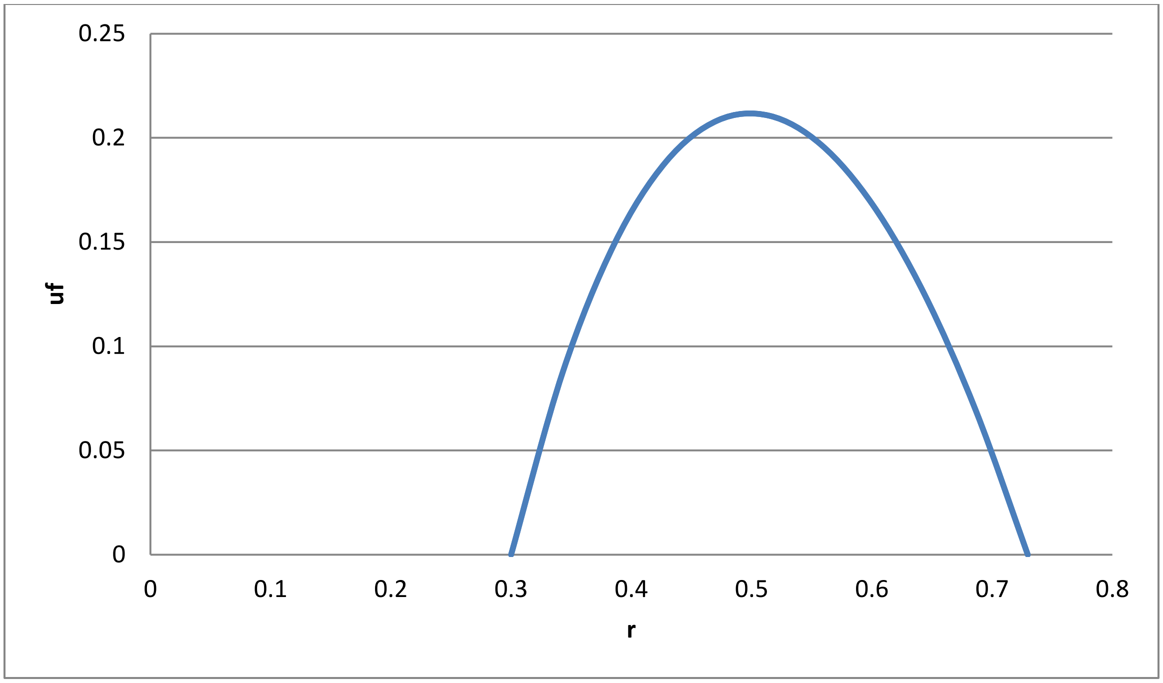

Figure 12. Plasma velocity versus radial variable for multi stenosis, z=2.5, C=0.5, r_1=0.3

Figure 13 shows the wall shear stress versus the axial variable for the multi-stenosis with hematocrit parameter C=0.1, 0.5 in the absence or presence of catheter. From this figure, it can be seen that wall shear stress is higher for hematocrit parameter C=0.5 in the presence of catheter with radius of 0.3 (r_1=0.3). In the case of no catheter, wall shear stress is the same for hematocrit parameter of 0.1 and 0.5. Wall shear stress does not vary outside the affected zone; however, the rate of increase of wall shear stress is significantly higher with severity of stenosis. Also, wall shear stress values are positive which indicates that it is acted by the blood flow on the artery.

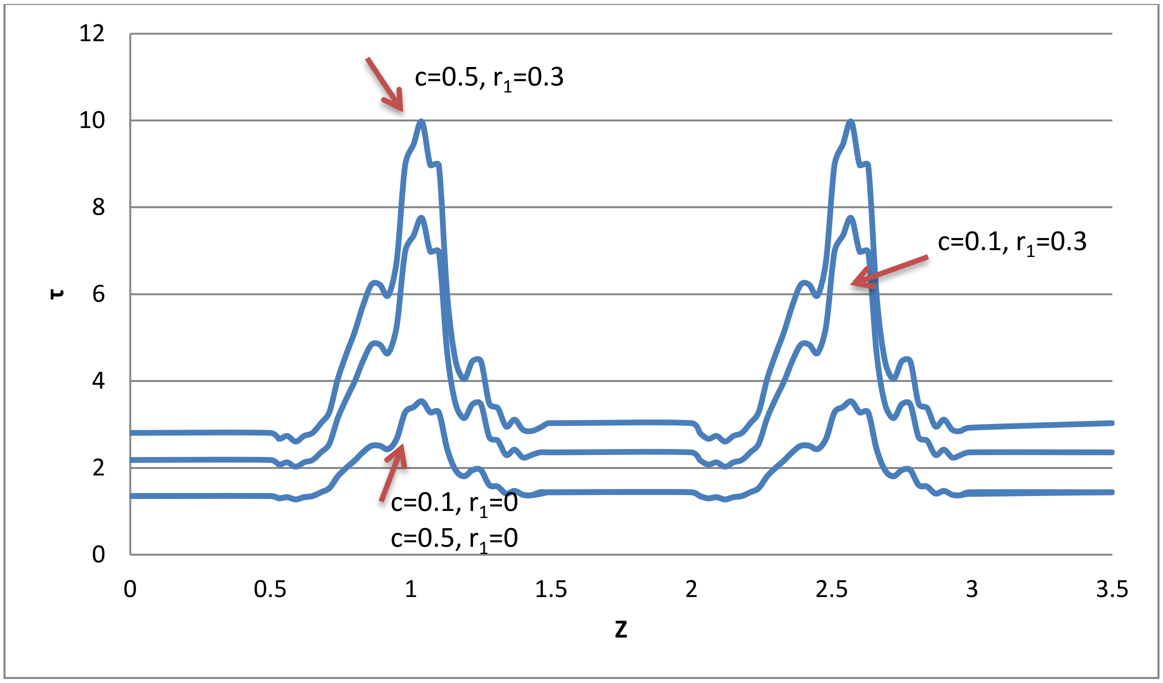

Figure 13. Wall shear stress versus *z* for *C*=0.1 (r_1=0, 0.3) and *C*=0.5 (r_1=0, 0.3).

Figures 14 and 15 present the wall stress force on the artery versus hematocrit with multi-stenosis in the absence or presence of catheter respectively. It can be seen from figure 14 that for small values of hematocrit, the stress force decreases with increasing hematocrit, and for larger values of hematocrit this stress force increases significantly. Figure 15 shows the same results but wall stress force is higher than wall stress force in absence of catheter.

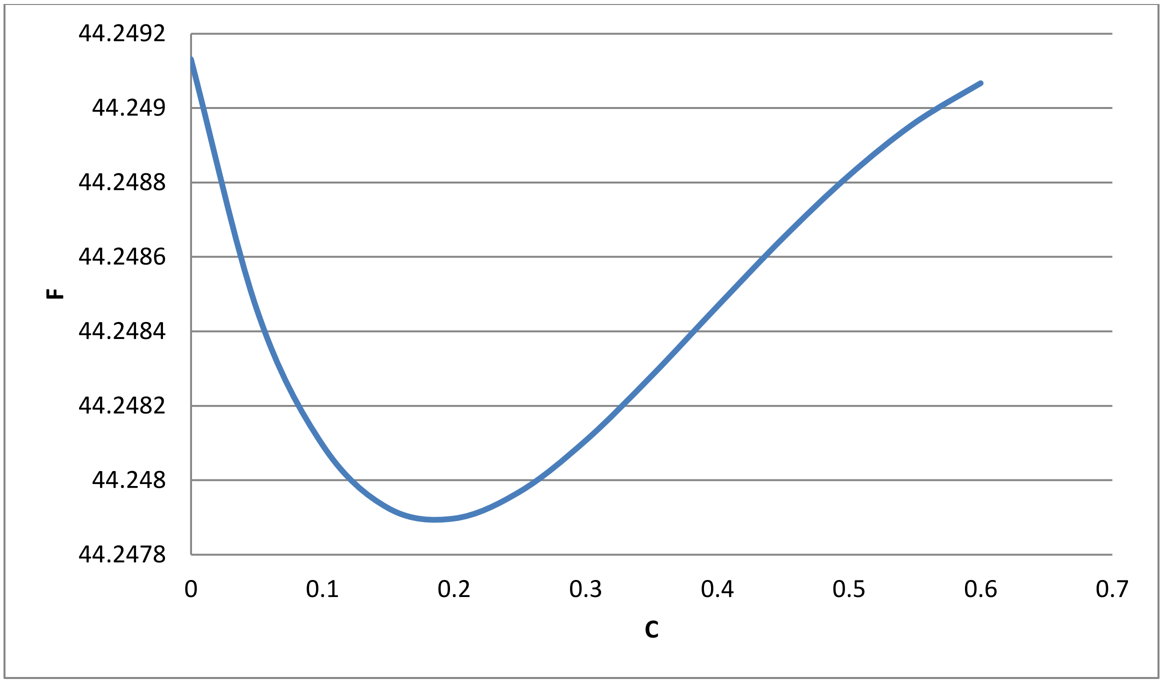

Figure 14. Stress force F versus C for r_1=0.

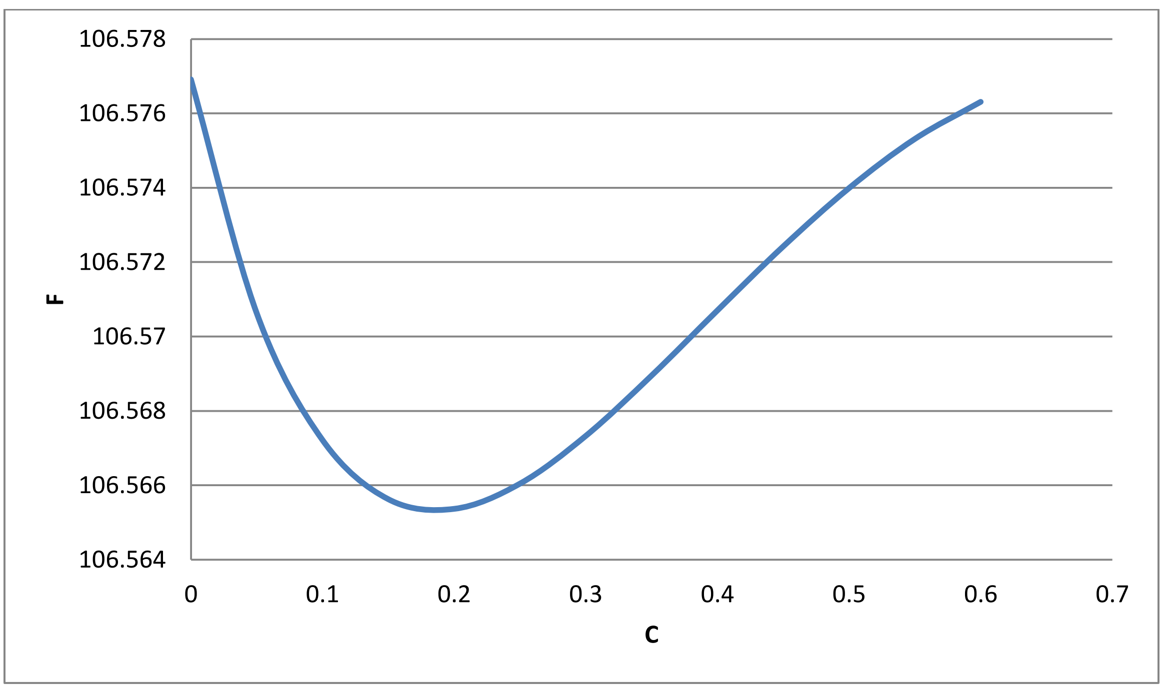

Figure 15. Stress force F versus C for r_1=0.3

Methodology of heat transfer and gravity effects in artery with single stenosis

The problem to be considered here will be a two-phase thermal flow system in a catheterized artery, which is assumed to be in an inclined position with respect to the horizontal level in order to take into account the effect of gravity. For this purpose, the steady axisymmetric forms of the equations in cylindrical coordinate system with axial direction along the co-axial direction of the catheterized artery are given by (Srivastava and Rastogi, 2010) for the mass conservation and momentum and by Smadi et al. (2006) for the temperature. They are given below

$$(1-C)\rho_f\left(u_f\frac{\partial u_f}{\partial z}+v_f\frac{\partial u_f}{\partial r}\right)=-(1-C)\frac{\partial P}{\partial z}+(1-C)\mu_s\nabla^2u_f-\rho_f g\sin(\alpha)(1-C)+CS'(u_p-u_f) \qquad (8a)$$

$$(1-C)\rho_f(u_f\frac{\partial v_f}{\partial z}+v_f\frac{\partial v_f}{\partial r})=-(1-C)\frac{\partial P}{\partial r}+(1-C)\mu_s(\nabla^2-\frac{1}{r^2})v_f-\rho_f g\cos(\alpha)(1-C)+CS'(v_p-v_f) \qquad (8b)$$

$$\frac{1}{r}\frac{\partial}{\partial r}[(1-C)v_f]+\frac{\partial}{\partial z}[(1-C)u_f]=0 \qquad (8c)$$

$$C\rho_P\left[u_p\frac{\partial u_p}{\partial z}+v_p\frac{\partial u_p}{\partial r}\right]=-\frac{\partial P}{\partial z}-C\rho_P g\sin(\alpha)+CS'\left(u_f-u_p\right) \qquad (8d)$$

$$C\rho_P\left[u_p\frac{\partial v_p}{\partial z}+v_p\frac{\partial v_p}{\partial r}\right]=-\frac{\partial P}{\partial z}-C\rho_P g\cos(\alpha)+CS'\left(v_f-v_p\right) \qquad (8e)$$

$$\frac{1}{r}\frac{\partial}{\partial r}(Crv_{p)}+\frac{\partial}{\partial z}\left(Cu_p\right)=0 \qquad (8f)$$

$$\rho_f C_h(1-C)^2\left(u_f\frac{\partial T}{\partial z}+v_f\frac{\partial T}{\partial r}\right)=\kappa(1-C)\nabla^2T+\mu_s(1-C)^2\ \{2[(\frac{\partial v_f}{\partial r})^2+(\frac{\partial u_f}{\partial z})^2+(\frac{v_f}{r})^2]+(\frac{\partial v_f}{\partial z}+\frac{\partial u_f}{\partial r})^2\} \qquad (8g)$$

Here $\nabla^2\equiv\frac{1}{r}\frac{\partial}{\partial r}\left(r\frac{\partial}{\partial r}\right)+\frac{\partial^2}{\partial z^2}$is the Laplace operator. Here *r, z, f, p, u, v, ρ, P, C,* μ_s are the same quantities used before, g is the acceleration due to gravity, α is the angle that the axis of the inclined artery makes with the horizontal direction, κ is the thermal conductivity of plasma, and

C_h is specific heat at a constant pressure. Formulas for viscosity of suspension μ_s and drag coefficient of interaction S' are also needed (Srivastava, 1996; Srivastava,2009)

$$\mu_s=\frac{\mu_0}{(1\text{-}mC)},\ m=0.07e^{2.49C+\frac{1107}{T}e^{-1.69C}} \tag{8h}$$

$$S'=4.5\frac{\mu_0}{a_0{}^2}\left(\frac{4+3\sqrt{8C\text{-}3C^2}+3C}{(2\text{-}3C)^2}\right) \tag{8i}$$

Where μ_0 is the plasma viscosity, a_0 is radius of a red cell and T is the absolute temperature in Kelvin. Figure 26 shows the flow system and the geometry is shown in an inclined cylindrical annulus, where the axis of the annulus is at angle α with respect to the horizontal level so that the effect of gravity can be taken into account. Similarly to the system discussed before, the catheterized arterial tube is given over a distance $L=2d_0+L_0$ in the axial direction, δ is the maximum height of the stenosis into the lumen, and the critical height is at a distance $z=d_0+L_0/2$ form the origin of the coordinate system.

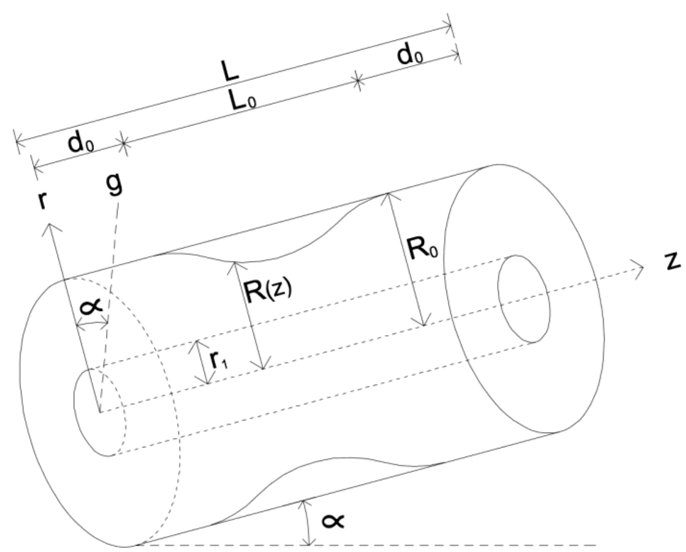

Figure 26. Artery system and geometry.

It is needed first to make the governing equations (8a-h) dimensionless using U, L_0, R_0, δ and $\mu_0 U L_0/\delta^2$, $(T_w - T_1)$ as scales for velocity, axial length, radial length, rate of radial change, pressure and temperature, respectively, where U is the maximum velocity for the unidirectional flow in a cylindrical annulus (White, 1991), T_w is the temperature on the surface of artery and T_1 is a reference temperature in the absence of the catheter, while in the presence of the catheter it is assumed to be the temperature on the surface of catheter. It is assumed that $T_w > T_1$. Next, simplify the dimensionless forms of the governing equations (8a-h) under the reasonable conditions for mild atherosclerosis with $\delta/R_0 << 1$, unidirectional flow assumption (White, 1991) where the axial velocity component dominates over the radial velocity component, and subjected the assumptions that the inertial terms in the governing momentum equations (8a-b, d-e) as well as convective terms in (8g) are small and $R_e\ (\delta/L_0) << 1$. Under these conditions and assumptions (Srivastava and Rastogi, 2010), the pressure is only a function of z and (8a-h) lead to simpler equations. These simpler equations in dimensionless form are given below using the same symbols for the variables as their dimensional ones for simplicity of notations, except that in the following equations $\theta \equiv (T-T_w)/(T_1-T_w)$ is used as the non-dimensional form of the difference between the plasma temperature and the temperature on the artery wall

$$(1\text{-c})\frac{dP}{dz}=\frac{1\text{-}C}{1\text{-}mC}\left[\frac{1}{r}\frac{\partial}{\partial r}\left(r\frac{\partial u_f}{\partial r}\right)\right]-\frac{1\text{-}C}{F_r}\sin(\alpha)+CS\beta^2\left(u_p\text{-}u_f\right) \tag{9a}$$

$$\frac{dP}{dz}=S\beta^2\left(u_f\text{-}u_p\right)-\frac{1}{F_r}\sin(\alpha),\quad S=4.5\left(\frac{4+3\sqrt{8C\text{-}3C^2}+3C}{(2\text{-}3C)^2}\right) \tag{9b}$$

$$\frac{1}{r}\frac{\partial}{\partial r}\left(r\frac{\partial\theta}{\partial r}\right)=E\frac{1\text{-}C}{1\text{-}mC}\left(\frac{\partial u_f}{\partial r}\right)^2 \tag{9c}$$

where $F_r = (\mu_0 U)/(g\ \rho_f\ \delta^2)$ is the Froude number, which is a non-dimensional parameter and inversely dependent on the gravity, $E=(U^2\mu_0)/[\kappa(T_w\text{-}T_1)]$ is an Eckert number , which is an equivalent parameter with product of Prandtl number and a regular Eckert number (Smadi et al., 2006), and $\beta=\delta/a_0$. The Eckert number represents the effect of the temperature.

For the artery flow with catheter, the equations (9a-c) are subjected to the following no slip boundary conditions

$$u_f = 0 \text{ and } \theta = 1 \text{ on } r = r_1;\ u_f = \theta = 0 \text{ on } r = R(z), \tag{9d}$$

while for the artery flow in the absence of the catheter, (2a-c) are subject to the following boundary conditions

$$\partial u_f/\partial r = \partial\theta/\partial r = 0 \text{ at } r = 0;\ u_f = \theta = 0 \text{ on } r = R(z). \tag{9e}$$

Using (9b) for ($u_f - u_p$) in (9a) and integrating twice with respect to r and making use of the boundary conditions given in (9d), it can be shown that

$$u_f = \left(\frac{-1}{4}\right)\left(\frac{1-mC}{1-C}\right)\left(\frac{dP}{dz} + \frac{\sin(\alpha)}{F_r}\right)\left[\left(R^2 - r^2\right) + \frac{\left(R^2 - r_1^{\,2}\right)\ln\left(\frac{r}{R}\right)}{\ln\left(\frac{R}{r_1}\right)}\right] \tag{10a}$$

In the limit of $r_1 \to 0$, this solution turns out to be also the solution satisfying (9e) for the case in the absence of the catheter.

The expression for the axial velocity for the red cells is then found from (9b) in terms of the axial velocity of the plasma in the form

$$u_p = u_f - \left(\frac{1}{S\beta^2}\right)\left(\frac{dP}{dz} + \frac{\sin(\alpha)}{F_r}\right) \tag{10b}$$

Since both expressions for the axial velocity of plasma and red cells given by (10a-b) are in terms of the unknown pressure gradient (dP/dz), pressure gradient can be obtained by assuming a prescribed volume flow rate in the annulus given by

$$Q = 2\pi \int_{r_1}^{R} r\left[(1-C)u_f + Cu_p\right]dr \tag{11}$$

Using (10a-b) in (11) and solving for the pressure gradient, it can be obtained

$$\frac{dP}{dz}=-\left(\frac{\sin(\alpha)}{F_r}\right)-\frac{Q}{\left(\frac{\pi}{16}\right)\left(R^2-r_1{}^2\right)\left\{\left(\frac{16C}{S\beta^2}\right)+2\left(\frac{R^2-r_1{}^2}{1-C}\right)(1-mC)\left[\frac{R^2+r_1{}^2}{R^2-r_1{}^2}-\frac{1}{\ln\left(\frac{R}{r_1}\right)}\right]\right\}} \tag{12}$$

In the limit of $r_1 \to 0$, the solution (12) represents the pressure gradient in the absence of the catheter. The flow resistance, referred to as the impedance λ, is given by

$$\lambda = \Delta P/Q, \tag{13a}$$

where Δp is the pressure drop across the length $1+2b$ given by

$$\Delta P=P(0)-P(L)=\int_0^{1+2b}\left(\frac{dP}{dz}\right)dz \tag{13b}$$

and $b=d/L_0$.

Using (9c), integrating twice with respect to r and making use of (9d), θ can be obtained and it is given by

$$\theta=EA^2\left(\frac{1-mC}{1-C}\right)\left\{\frac{1}{4}r^4-\frac{\left(R^2-r_1{}^2\right)r^2}{\ln\left(\frac{R}{r_1}\right)}+\frac{\left(R^2-r_1{}^2\right)^2\ln(r)^2}{2\left(\ln\left(\frac{R}{r_1}\right)\right)^2}+c_1\ln(r)+c_2\right\} \tag{14a}$$

where

$$A=\frac{1}{4}\left(\frac{1-mC}{1-C}\right)\left(\frac{dP}{dz}+\frac{\sin(\alpha)}{F_r}\right),\ c_1=\frac{c_3-c_4}{\ln\left(\frac{R}{r_1}\right)},\ c_2=c_3-c_1\ln(R),$$

$$c_3=-\frac{1}{4}R^4+\frac{\left(R^2-r_1{}^2\right)R^2}{\ln\left(\frac{R}{r_1}\right)}-\frac{\left(R^2-r_1{}^2\right)^2\ln(R)^2}{2\left(\ln\left(\frac{R}{r_1}\right)\right)^2},\ c_4=-\frac{1}{4}r_1{}^4+\frac{\left(R^2-r_1{}^2\right)r_1{}^2}{\ln\left(\frac{R}{r_1}\right)}-\frac{\left(R^2-r_1{}^2\right)^2\ln(r_1)^2}{2\left(\ln\left(\frac{R}{r_1}\right)\right)^2}+\frac{1}{EA^2} \tag{14b}$$

In order to calculate the total heat flux on the surface of the artery, first (14a) is used to determine the radial rate of change of θ on the artery surface which is given below

$$\frac{\partial\theta}{\partial r}\Big|_{r=R(Z)}=EA^2\left(\frac{1-C}{1-mC}\right)\{r^3+\frac{2\left(r_1{}^2-R^2\right)}{\ln\left(\frac{R}{r_1}\right)}+\frac{\left(R^2-r_1{}^2\right)^2\ln(r)}{r\left(\ln\left(\frac{R}{r_1}\right)\right)^2} \tag{15a}$$

which can hold also in the case without the catheter if the limit of $r_1 \to 0$ is taken. The heat flux q over surface of the artery from z=0 to z=1+2b is then given by

$$q=2\pi \int_0^{1+2b} \left[\frac{\partial \theta}{\partial r}\Big|_{r=R(z)}\right] dz = 2\pi E \left(\frac{1-mC}{1-C}\right) \int_0^{1+2b} A^2 c_5 dz \tag{15b}$$

where

$$c_5=R^3-\frac{2R\left(R^2-{r_1}^2\right)}{\ln\left(\frac{R}{r_1}\right)}+\frac{\left(R^2-{r_1}^2\right)^2 \ln(R)}{R\left(\ln\left(\frac{R}{r_1}\right)\right)^2}+\frac{c_1}{R} \tag{15c}$$

Calculations using the previous expressions are introduced for different values of hematocrit C, and different values for radius of catheter, and in the absence of catheter. For all calculations, Q=1, b=0.5, α=45° and β=δ/0.004 where δ=1-minimum value of R. (Garcia, Riahi 2013)

Figure 16 represents the pressure gradient dP/dz versus the axial variable Z for single stenosis where C=0.3 was used as the hematocrit, F_r=0.1, 0.2 and for absence of catheter (r_1=0). From this figure, one can notice that the blood pressure gradient is negative which makes sense since the blood pressure force is in the positive direction of the z-axis. Also, it can be seen that if the Froude number is smaller, the magnitude of the blood pressure force is higher implying that the effect of gravity can increase the magnitude of such force. Also, it can be shown that for values of α between 0°<α<90°, the magnitude of pressure gradient increases, and it will decrease for values of α between -90°<α<0°. It can be also shown from the figure that the pressure gradient does not vary outside the stenosis zone; however it increases with the stenosis effect in the stenosis zone.

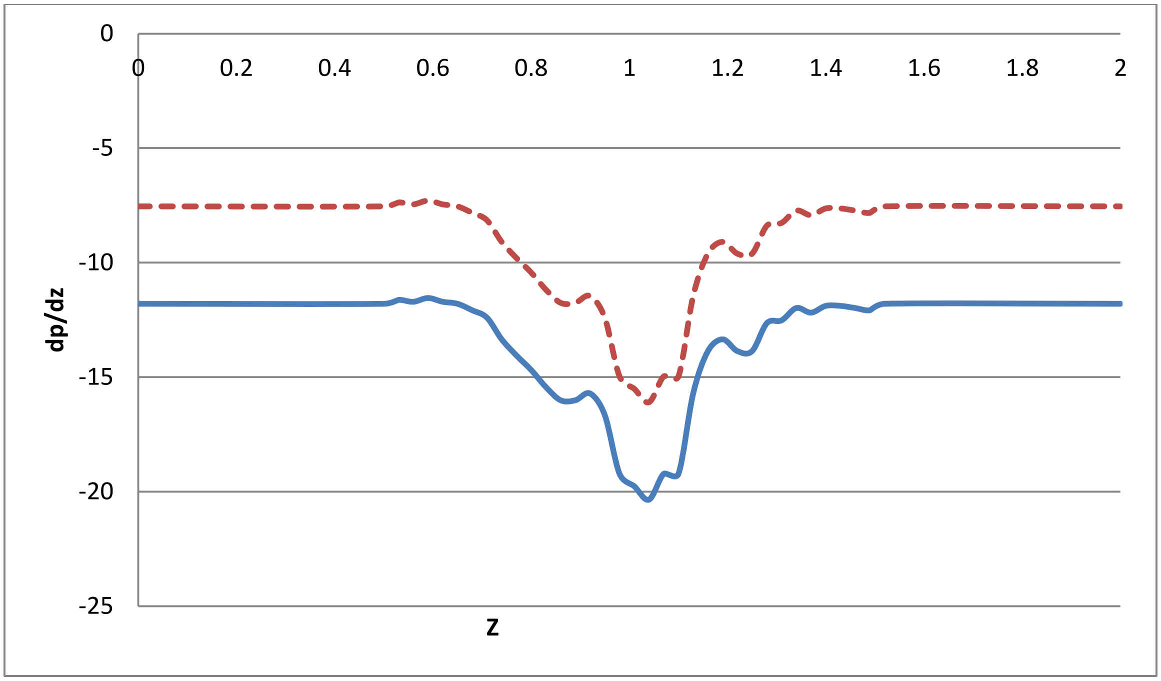

Figure 16. d*P*/dz versus *z* for r_1 =0, *C*=0.3, F_r=0.1 (solid line) and F_r=0.2 (dashed line).

Figure 17 shows the same results for figure 16 but now in the presence of catheter (r_1 =0.3). It can be seen that the magnitude for pressure gradient is higher when a catheter is inserted. Also, additional generated data shows that magnitude of blood pressure force in the artery increases with catheter radius which is reasonable since when a catheter is inserted it leads to smaller annulus gap leading to higher values of such force.

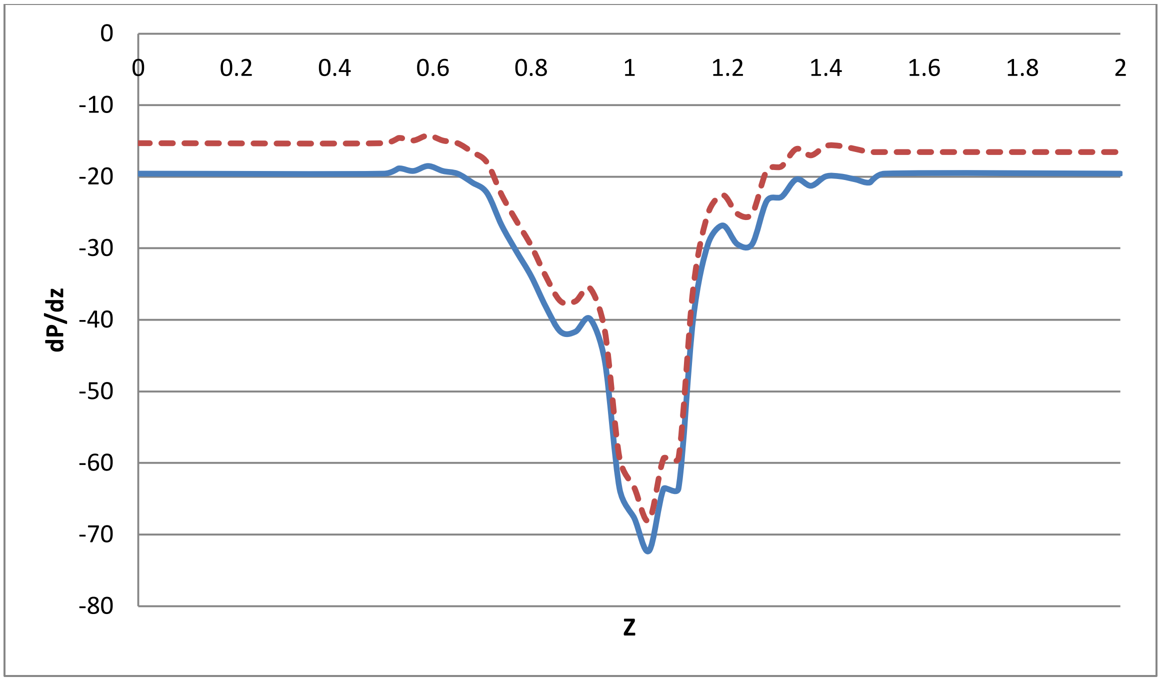

Figure 17. d*P*/dz versus *z* for r_1 =0.3, *C*=0.3, F_r=0.1 (solid line) and F_r=0.2 (dashed line).

Data for axial velocity of blood plasma versus the axial variable for different values of hematocrit and in the absence or presence of catheter is also calculated. It can be seen that plasma velocity does not vary outside the stenosis zone; however its magnitude increases with the stenosis effect. Also, plasma velocity is positive since the blood pressure force is in the positive direction of the axis of the artery system. Bio-medically, this is reasonable since for higher stenosis, the pressure force increases leading to higher blood plasma speed. The plasma velocity increases significantly with larger radius of catheter which is reasonable since higher catheter radius decreases the annulus gap leading to higher plasma speed.

Concerning the effect of the gravity on the plasma velocity, the expression for the axial velocity of the plasma indicated that the effect of gravity even though is notable for the pressure gradient; it is cancelled out for the axial velocity. This is reasonable physically since in the presence of gravity the pressure gradient generates additional value to counteract the presence of the gravity force component along the axial direction leading to zero effect of the gravity on the plasma velocity (Garcia, Riahi 2013).

Figures 18-21 shows the difference between the blood temperature and the temperature on the artery wall (θ) versus the axial variable (z) with r=0.5 and radial variable (r) with z=1 in the absence or presence of catheter with hematocrit parameter of 0.3, E=0.2,0.6. It can be seen from these figures that the blood temperature is higher than the temperature on the artery wall in the absence of catheter. However, in the presence of a catheter (r_1=0.3), the blood temperature is lower than the temperature on the artery wall which indicates that the blood zone is smaller in the presence of the catheter leading to smaller viscous heating and so the artery temperature exceeds blood temperature. Additional generated data for the blood temperature versus the hematocrit parameter indicates that the blood temperature variation with respect to the hematocrit effect is insignificant. The expressions for θ for both cases in presence and absence of the catheter indicate that the effect of the gravity is zero on the temperature which is consistent physically since gravity was found to have no effect on the plasma velocity and hence no effect on the viscous heating and, thus, no effect on the temperature profile (Garcia, Riahi 2013).

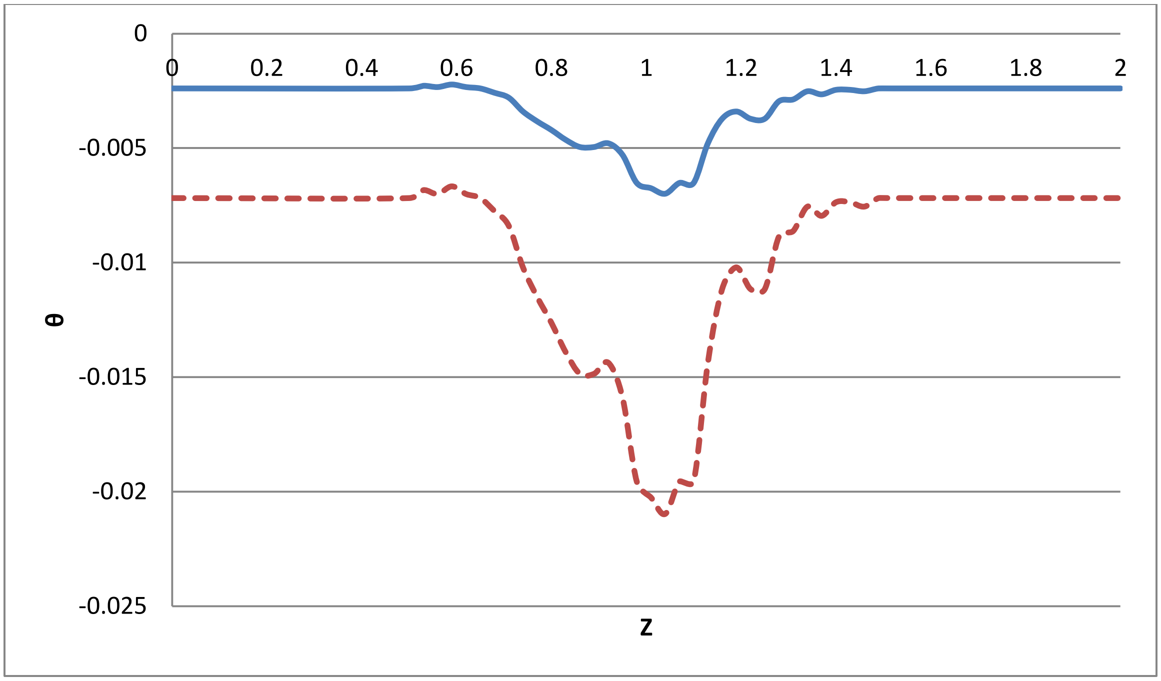

Figure 18. θ versus *z* in the artery with no catheter for *C*=0.3, *r*=0.5, *E*=0.2 (solid line) and *E*=0.6 (dashed line).

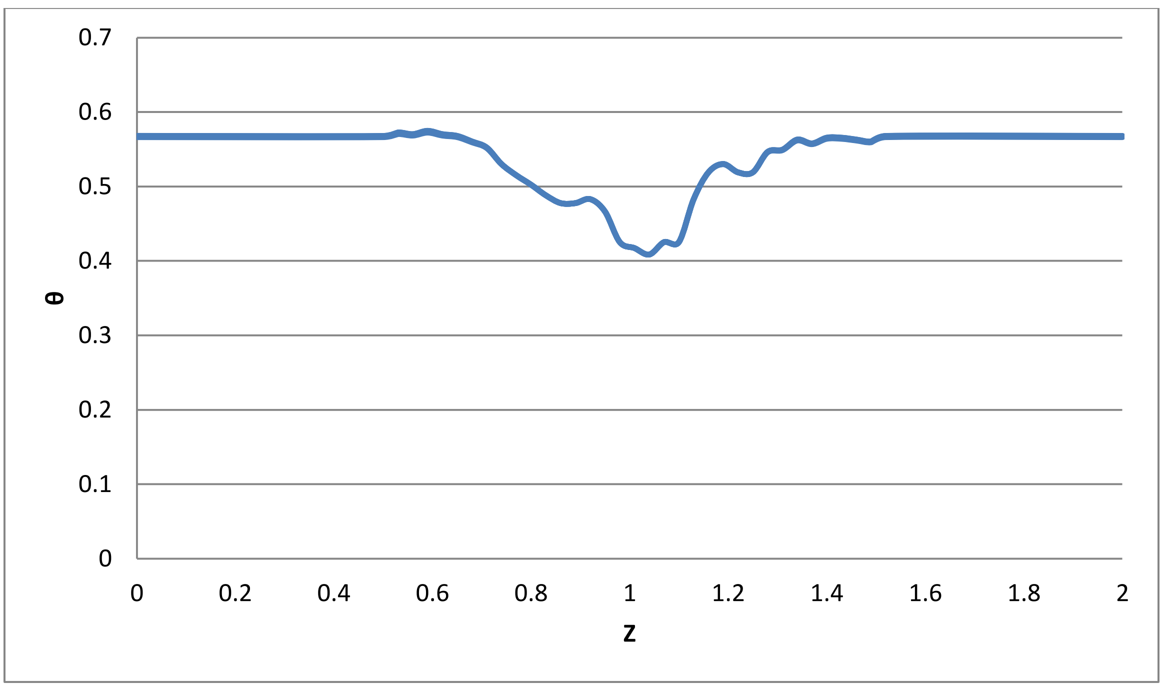

Figure 19. θ versus *z* for the artery with catheter, *C*=0.3, *r*=0.5 and *E*=0.2.

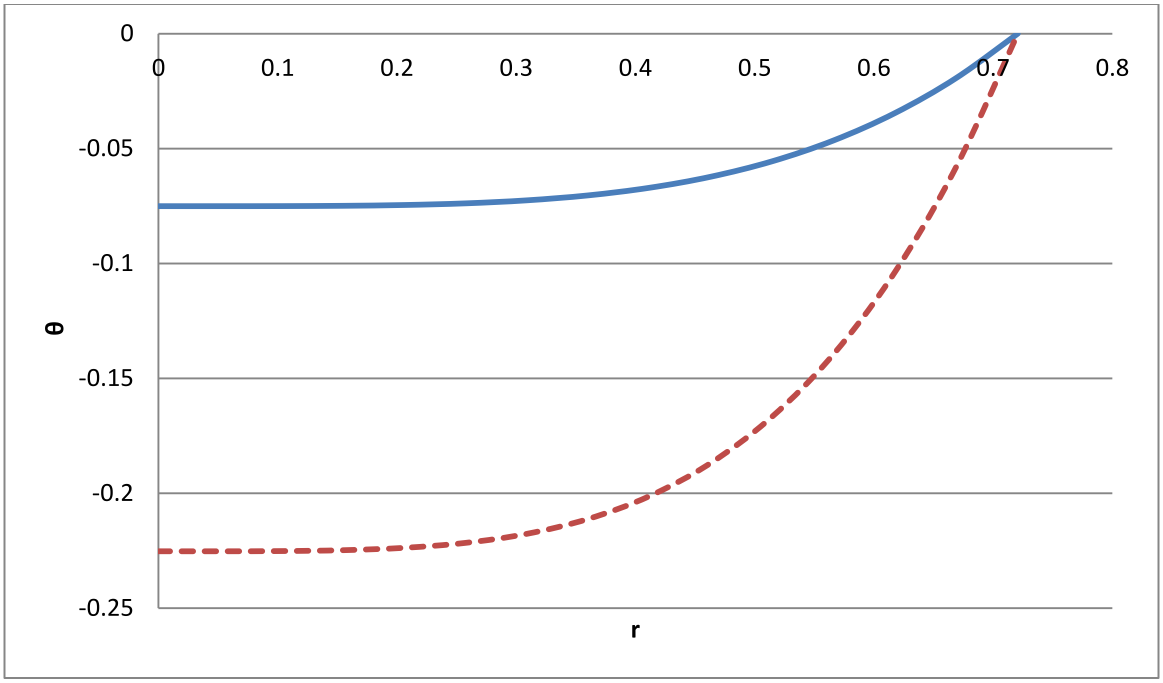

Figure 20. θ versus r for r_1 =0, C=0.3, z =1, E=0.2 (solid line) and E=0.6 (dashed line).

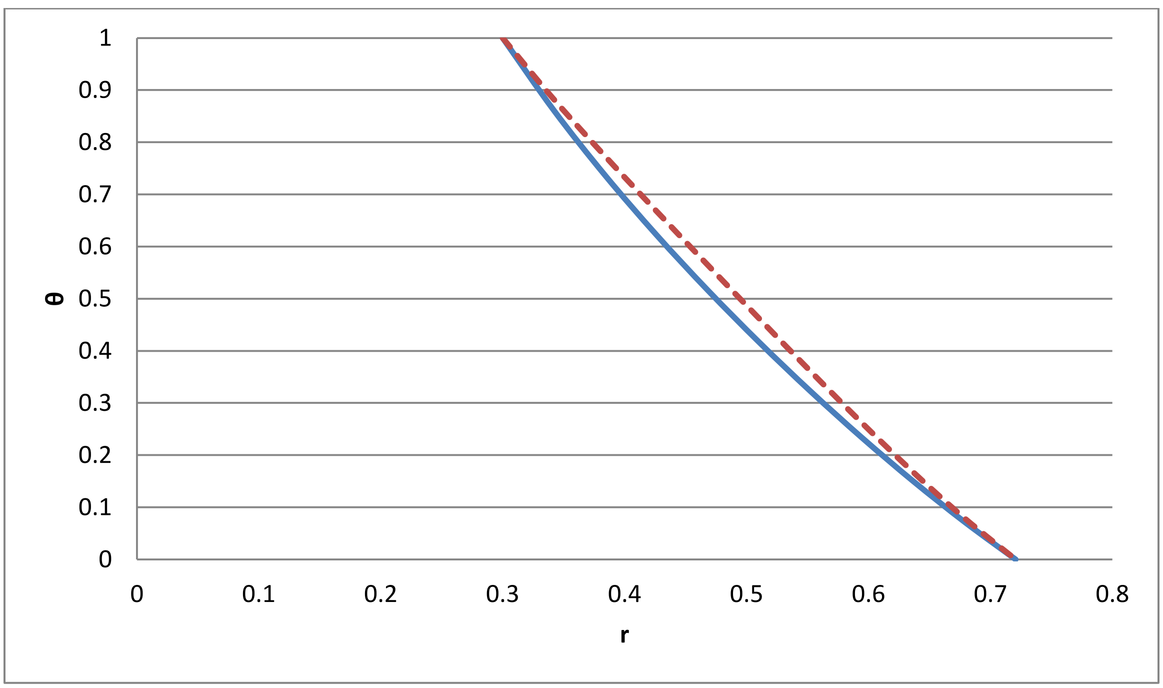

Figure 21. θ versus r for r_1=0.3, C=0.3, z =1, E=0.2 (solid line) and E=0.6 (dashed line).

Figure 22 and 23 presents the flow resistance also known as impedance versus hematocrit parameter in the absence or presence of catheter for $F_{r=}$0.1and 0.2. It can be seen from these two figures that impedance increase linearly with the increase of the hematocrit parameter. Also, impedance increases in the presence of catheter (r_1=0.3) and it also increases with the effect of gravity.

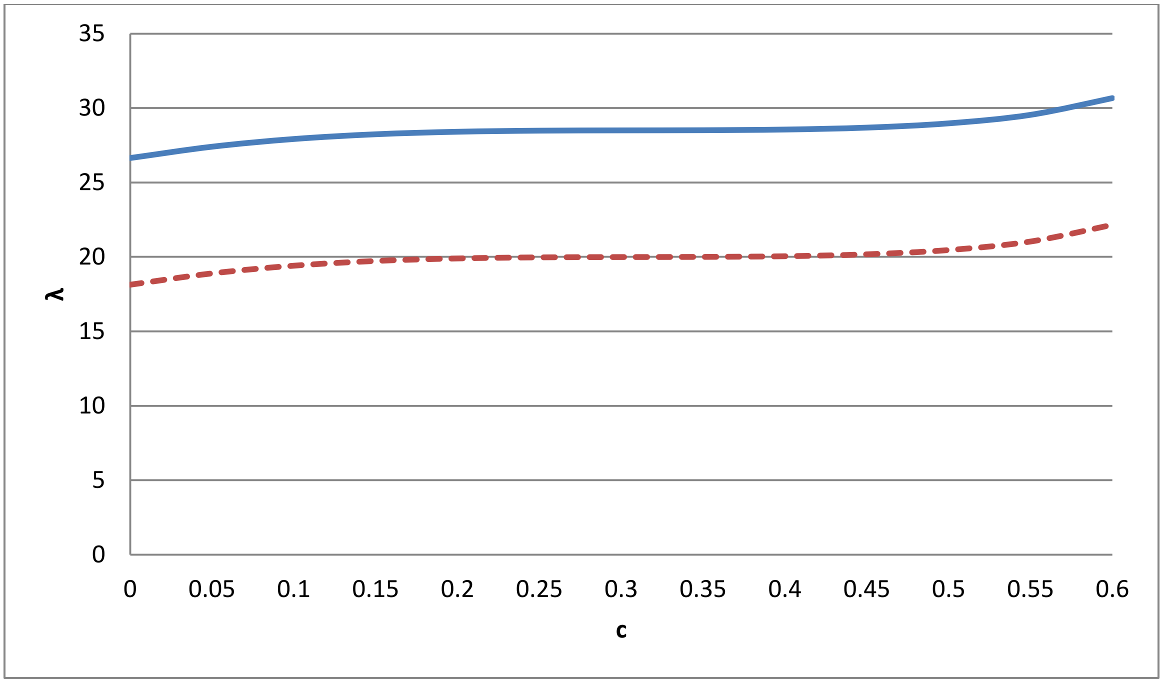

Figure 22. Impedance λ versus C for r_1 =0, F_r= 0.1 (solid line) and F_r= 0.2 (dashed line).

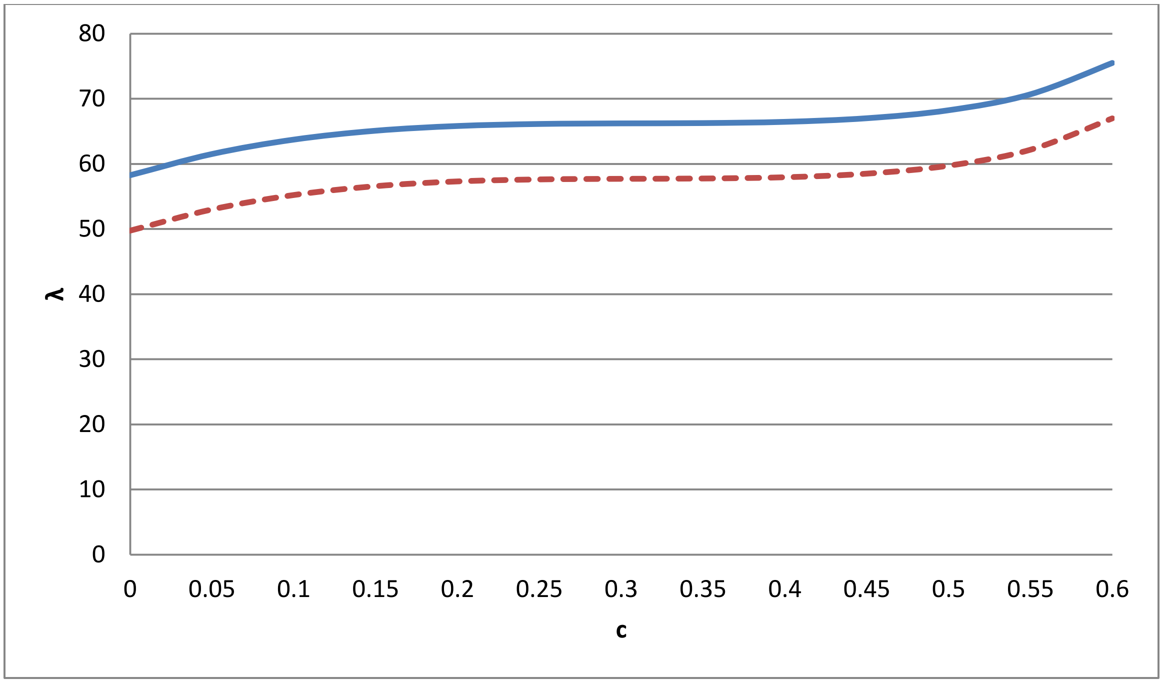

Figure 23. Impedance λ versus C for r_1 =0.3, F_r= 0.1 (solid line) and F_r= 0.2 (dashed line).

Figures 24-25 show the heat flux q versus hematocrit parameter in the absence or presence of catheter with E=0.2, 0.6. It can be seen that heat flux increases linearly with increasing of hematocrit parameter. In figure 24, for absence of catheter, it can be seen that the heat flux is positive implying that the flow of heat goes from the blood zone to the outside of the artery. However, figure 25 shows that for presence of catheter, the heat flux is negative which indicates that heat flow goes from outside of the artery into the blood zone. In addition, the magnitude of the heat flux is higher in the presence of catheter.

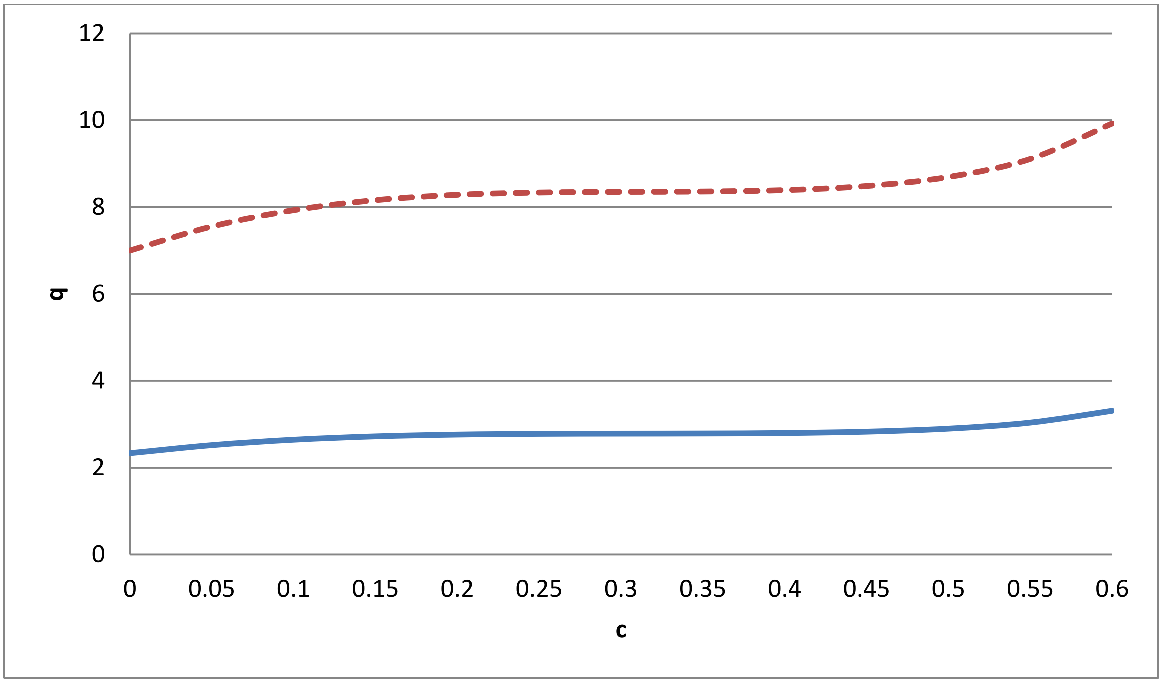

Figure 24. Heat flux *q* versus *C* for r_1=0, *E*=0.2 (solid line) and *E*=0.6 (dashed line).

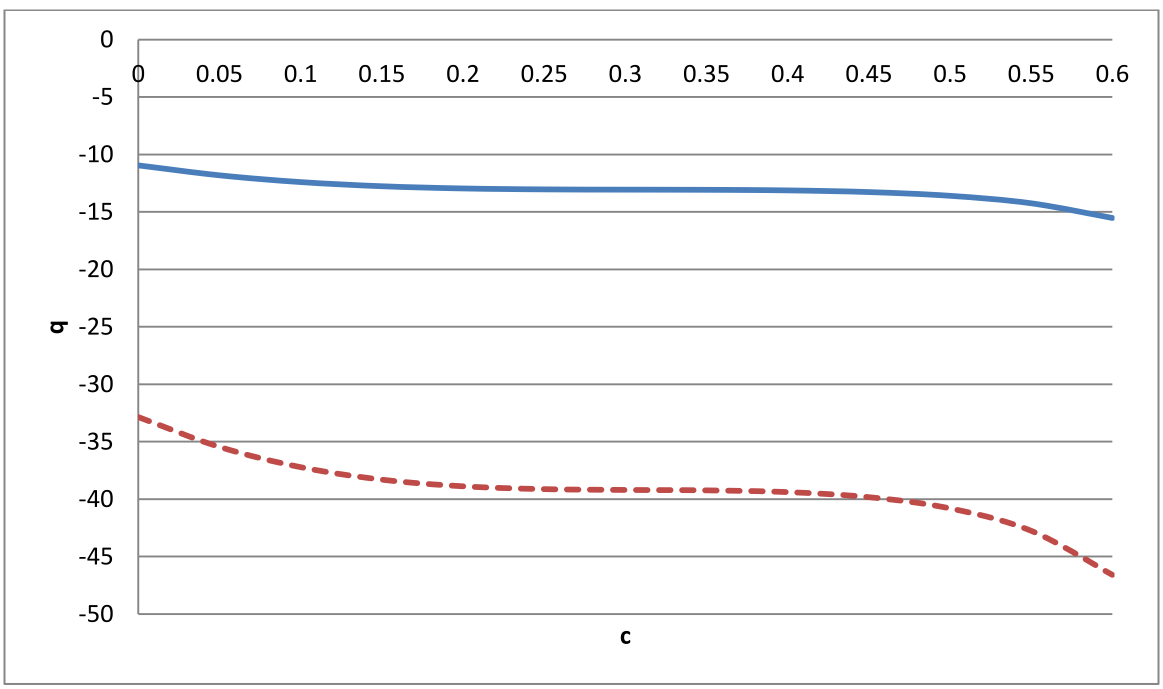

Figure 25. Heat flux *q* versus *C* for r_1=0.3, *E*=0.2 (solid line) and *E*=0.6 (dashed line).

CHAPTER IV

SUMMARY AND CONCLUSION

First, arterial two-phase blood flow with or without a catheter in the presence of single or multiple stenosis was investigated. The modeling for the stenosis was based on the available experimental data for a human's artery with stenosis. Important quantities were calculated, such as the pressure gradient force, the plasma velocity, the impedance, the wall shear stress and the wall stress force in the artery which contained either a single or multiple stenosis zones and in the presence or absence of the catheter. It was found that pressure gradient force, plasma velocity, impedance, wall shear stress and wall stress force increase with increasing the hematocrit if percentage of red cells in plasma is too small. In addition, it was shown that in the presence of catheter, the plasma speed, magnitude of pressure gradient, wall shear stress, stress force and impedance increase.

Also, effects due to the presence of gravity and heat transfer in arterial blood blow system for single stenosis were taken into consideration. And quantities such as pressure gradient force, flow velocity, impedance, and blood temperature and wall heat flux were calculated. It was found that that the force gravity introduce additional contribution in the pressure gradient which can enhance the blood pressure force for upslope direction of the artery, while it can reduce the effect of the blood pressure force in the case of down-slope artery. The effect of viscous heating leads to heat flow out of the blood zone for the artery system in the absence of the catheter, while the heat flow is into the blood zone in the presence of the catheter. It is also found that the pressure gradient force, flow velocity and the impedance are stronger in the stenosis. In addition the magnitude of the heat flux increases with the hematocrit parameter. These conditions could be relevant to the corresponding conditions for certain patients, which can require higher care and attention (Garcia, Riahi 2013)

REFERENCES

Back, L. H., Cho, Y. I., Crawford, D. W. and Cuffel, R. F., (1984), Effect of mild atherosclerosis on flow resistance in a coronary artery casting of man, Transactions of the ASME, 106, 48-53

Back, L. H., (1994), Estimated mean flow resistance during coronary artery catheterization, *Journal of Biomechanics*, 27, 169-175

Back, L. H., Kwack, E. Y. and Back, M, R., (1996), Flow rate-pressure drop relation to coronary angioplasty: Catheter obstruction effect, *Journal of Biomedical Engineering*, 118, 83-89

Batchelor, G, (1970), An Introduction to Fluid Dynamics, Cambridge University Press, UK

Charm, S. E., Kurland, G. S., (1974), Flow and Microcirculation, John Wiley, New York.

Kanai, H., Lizuka, M. and Sakamotos, K., (1970). One of the problem in the measurement of blood pressure by catheterization: Wave reflection at the tip of catheter, Med. Biol. Engr., 28, 483-496

Mishra, B K., (2003). A mathematical model for the analysis of blood flow in arterial stenosis, The Mathematics Education, 37, 176-181.

Mishra, B K. and Panda, T C, (2005). Non-Newtonian model of blood flow through an arterial stenosis, Acta Ciencia Indica, 31 M(2): 341-348.

Riahi, D. N., Roy, R. and Cavazos, S., (2011) On arterial blood flow in presence of an overlapping stenosis, Mathematical and Computer Modeling, 54, 2999-3006

Smadi, O., Packirisamy, M., Stiharu, I. and Rakheja, S., (2006) Modeling of blood flow through multi-stenosis arteries, IEEE-ISIE, July 9-12, 2006, 3400-3403.

Srivastava, V. P., (1996). Two-phase model of blood flow through stenosed tubes in the presence of a peripheral layer: Applications, *Journal of Biomechanics*, 29, 1377-1382.

Srivastava, V. P., Srivastava, R., (2009) Particulate suspension blood flow through a narrow catheterized artery, Comput. Math. Appl., 58, 227-238.

Srivastava, V P, Rastogi, R and Mishra, S, (2010) Non-Newtonian arterial blood flow through an overlapping stenosis, Applications and Applied Math: An Int. Journal, 5 (1): 225-238.

Srivastava, V. P. and Rastogi, R., (2010) Blood flow through a stenosed catheterized artery: Effects of hematocrit and stenosis shape, Computer and Mathematics with Applications, 59, 1377-1385.

Tam, C. K. W., (1969). The drag on a cloud of spherical particles in low Reynolds number flows, *Journal of Fluid Mechanics*, 38, 537-546.

Venkateswarlu, K and Rao, J A, (2004). Numerical solution of unsteady blood flow through an indented tube with atherosclerosis, *Indian Journal of Biochemistry and Biophysics*, 41, 241-245.

White, F. M., (1991). Viscous Fluid Flow, Second Edition, McGraw-Hill, Inc., New York.

Young, D F and Tsai, F Y, (1973). Flow characteristics in model of arterial stenosis-steady flow, *J. Biomechanics*, **6**: 395-410.

Riahi D.N., Garcia A.E., (2013) Two-phase arterial blood flow with or without a catheter and in the presence of single or multi stenosis. (Submitted)

Riahi D.N., Garcia A.E., (2013) Two-phase blood flow and heat transfer in an inclined stenosed artery with or without a catheter. (Submitted)

BIOGRAPHICAL SKETCH

Ani Emire Garcia Escorcia was born in Rio Bravo, Tamaulipas, Mexico. Ani completed her bachelor's degree on Applied Mathematics at the University of Texas Pan American in May 2011. During her time in college, she worked as student assistant for the Quality Enhancement Program (QEP) for two years in the math department. After finishing her degree, she started her master on Mathematical Science. At the same time she worked as a Graduate Teaching Assistant in the math department at UTPA. After two years of hard working, she completed her master degree on Mathematical Science in May 2013.

Ani Emire Garcia Escorcia

804 Russian Ave. Apt 1

Edinburg, TX. 78539

Phone: (956)-502-1901